



**HAL**  
open science

## Dielectric properties of segmented polyurethanes for electromechanical applications

M.H. Jomaa, L. Seveyrat, L. Lebrun, K. Masenelli-Varlot, J.Y. Cavaille

► **To cite this version:**

M.H. Jomaa, L. Seveyrat, L. Lebrun, K. Masenelli-Varlot, J.Y. Cavaille. Dielectric properties of segmented polyurethanes for electromechanical applications. *Polymer*, 2015, 63, pp.214-221. 10.1016/j.polymer.2015.03.008 . hal-01769257

**HAL Id: hal-01769257**

**<https://hal.science/hal-01769257>**

Submitted on 14 Jun 2019

**HAL** is a multi-disciplinary open access archive for the deposit and dissemination of scientific research documents, whether they are published or not. The documents may come from teaching and research institutions in France or abroad, or from public or private research centers.

L'archive ouverte pluridisciplinaire **HAL**, est destinée au dépôt et à la diffusion de documents scientifiques de niveau recherche, publiés ou non, émanant des établissements d'enseignement et de recherche français ou étrangers, des laboratoires publics ou privés.

# **Dielectric properties of segmented polyurethanes for electromechanical applications**

M. H. Jomaa<sup>1,2\*</sup>, L. Seveyrat<sup>2</sup>, L. Lebrun<sup>2</sup>, K. Masenelli-Varlot<sup>1</sup>, J.Y. Cavaille<sup>1</sup>.

<sup>1</sup> Materials, Engineering and Science Lab, MATEIS, INSA-Lyon, UMR CNRS 5510, Université de Lyon, F-69621 Villeurbanne Cedex, France

<sup>2</sup> Laboratory of Electrical Engineering and Ferroelectricity, LGEF INSA Lyon EA682, Université de Lyon, F-69621 Villeurbanne Cedex, France

\* Author to whom all correspondence should be addressed

## **Abstract**

The paper deals with electromechanical and dielectric properties of polyurethanes (PU) block-copolymers. Most of the works published in the literature only consider electrostriction at room temperature at a given frequency. In this work, it is shown that electrostrictive coefficient  $M_E$  is divided by 3 to 10 at increasing frequency over 3 decades of frequency, depending on the ratio of hard to soft segments in PU. Thus it is important to analyze the energy conversion efficiency by investigating the dielectric and viscoelastic properties. This work deals with the study of dielectric properties of 3 PU with different fractions of hard segments. Three relaxation phenomena ( $\beta$ ,  $\alpha$  and conduction) were investigated for each PU in the temperature-frequency range studied here, in order to optimize the copolymer composition in view of their best efficiency as actuators or mechanical energy harvesting devices.

**Keywords:** EAP, Polyurethane, Electrostriction, Hard and soft segment, Dielectric relaxation

## I. Introduction

Electroactive polymers are one of the most promising technologies. Compared to inorganic materials, these versatile polymers have various attractive properties, such as being lightweight, inexpensive and easy to manufacture into any desirable shape. Tremendous amounts of research and development have led to Electroactive Polymers (EAP) that can change in size or shape when stimulated by an external electrical field, meaning they can convert electrical energy into mechanical energy [1]. Among the various EAPs, polyurethane (PU) elastomers are of great interest due to the significant electrical-field strains [2, 3, 4], and due to their attractive and useful properties, such as abrasion resistance, high mechanical strength and biocompatibility with blood and tissues [5]. The PU elastomers studied here are block copolymers of soft and hard segments (SS and HS). In this study, the hard segments (HS) are composed of 4,4'-methylene bis (phenyl isocyanate) (MDI) and 1,4-butanediol (BDO), whereas poly(tetramethylene oxide) is employed as soft segments (SS). It is worthy to notice that HS and SS are not miscible, and during the process, a partial phase separation occurs leading to the formation of soft domains (SD) rich in SS and hard domains (HD) poor in SS. This phase separation is limited because of the relatively low molecular weight of SS and HS blocks which prevents the entropy of mixing to decrease too much [6,7]. Furthermore, a slight crystallization can grow inside SD and HD. All of these parameters, namely the crystallinity ratio, the SD and HD topology, composition and concentration influence properties such as hardness, stiffness, and tensile strength [8]. It is well documented that the properties and the performances of polyurethanes are strongly dependent on the degree of microphase separation and on the ensuing morphologies [9, 10, 11, 12]. The objective of this present study is to highlight the strain thickness frequency dependence and to investigate the effect of the chemical composition through the HS content on the dielectric behavior of three different pure segmented PU, where the weight fraction of HS is varied. In order to achieve our goal, dielectric spectroscopy measurements were performed in a wide range of temperature and frequencies.

## II. Materials and methods

The studied polymers are polyether-based thermoplastic polyurethanes. They are co-block polymers with two major blocks: HS and SS. HS are composed of 4,4' methylene bis (phenyl isocyanate) (MDI) and 1,4-butanediol (BDO). Poly (tetramethylene oxide) (PTMO) is used as SS. The structure of PU is presented in Fig. 1.

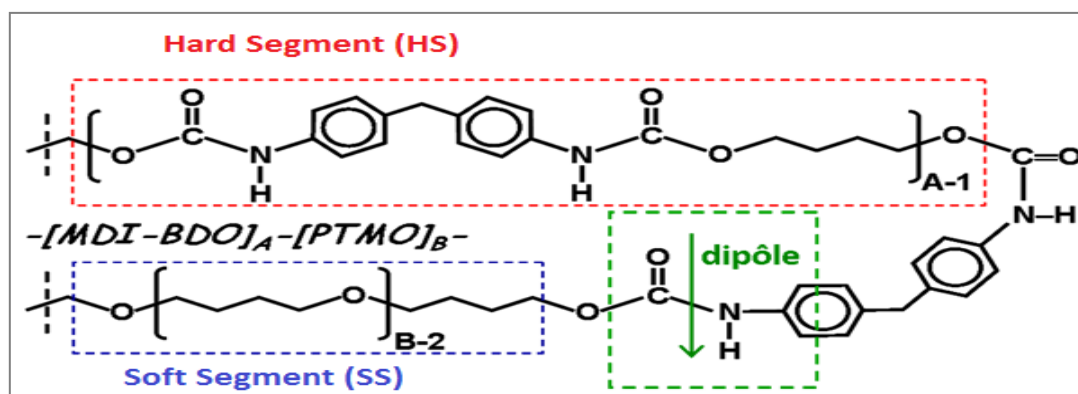


Fig. 1 Structure of the polyurethane consisting of MDI-BDO hard segments and PTMO soft segments [13].

The three different types of PU are commercially available and provided by the same company Lubrizol. They are synthesized by the same industrial process from the same initial chemical components. They differ in their weight fractions of HS: 26% for PU 75 (Estane X-4977), 45% for PU88 (Estane 58888 NAT021) and 65% for PU60 (Estane ETE60DT3 NAT022), and in different molecular weights of PTMO SS; 1000 g/mol for PU88, PU60 and 2000 g/mol for PU75.

The SS originate from the polyol and are responsible for the elastomeric behaviour of the polymeric material; the HS contain highly polar urethane linkages and it is thought [14, 15, 16,17] that due to phase separation they form highly polar and stiff microdomains embedded in a soft poorly polar matrix. Essentially, the morphology of the segmented polyurethanes depends on the relative amount of the soft and hard segments and on other physical phenomena such as crystallization and hydrogen bonds formation between the two types of segments.

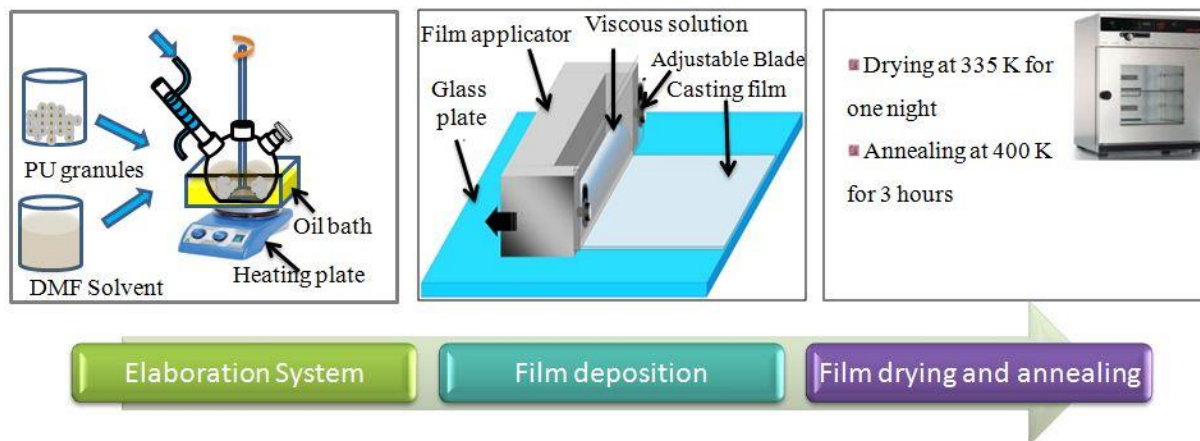


Fig. 2 Elaboration protocol of polyurethanes polymers.

The polymer films were prepared by solution casting. The elaboration process steps are described in the Fig. 2. Before use, PU granules were heated at 350 K for 3 hours. Then they were dissolved in N,N-dimethylformamide (DMF, Sigma-Aldrich D158550, 99%) with a ratio of 25% weight of PU into DMF. The solution was heated at 350 K for 4 hours under mechanical agitation, until a homogeneous solution was obtained. This operation was carried out in a closed device, to avoid evaporation of the DMF solvent and ensure good reproducibility of films.

The solution was then kept overnight to remove air bubbles. Afterwards, this solution was cast on glass plates with an Elcometer 3700 doctor blade film applicator Fig. 2, put in an oven at 335 K for one day, and then removed from the glass. A second heating treatment at a temperature below the HS melting temperature was performed in order to eliminate the residual solvent. The thickness of the films was 100  $\mu\text{m}$  after drying.

Glass transition and melting temperatures were determined with Differential Scanning Calorimetry (Setaram, DSC 131 Evo)) under nitrogen flow ( $P = 1.5$  bar). Samples of 20 mg were cooled by liquid nitrogen to 140 K and then heated to 480 K before being cooled to room temperature. The heating and cooling rates were set at 10 K / min.

The field-induced thickness strain  $S$  was measured on circular samples (25mm of diameter) with a homemade setup based on a double-beam laser interferometer measurement (Agilent 10889B) [4]. Samples were placed between two cylindrical brass mass acting as conductive electrodes. A mirror was placed on the upper electrode to reflect the laser beam. A bipolar

electric field was supplied by a high voltage amplifier (Trek10/10B) driven with a function generator (Agilent 33250A). Measurements were made at room temperature on samples of 100  $\mu\text{m}$  of thickness.

The dielectric properties of these films were measured with a Modulab MTS at an AC voltage of 1 VRMS, over a frequency range of  $10^{-1}$  to  $10^5$  Hz. Both surfaces of the film -of 100 $\mu\text{m}$  of thickness- were coated with a gold electrode of 20 mm in diameter, deposited by sputtering (Cressington 208 HR). The real and imaginary parts of the dielectric permittivity  $\epsilon^*$  and of the conductivity  $\sigma^*$  were obtained. The complex dielectric modulus,  $M^* = \frac{1}{\epsilon^*}$  was also determined as explained below. Isothermal measurements were performed under liquid nitrogen using a cryostat (JANIS-STVP-200XG), in the temperature range 180 K to 380 K. Dielectric relaxation, activation energy and characteristic relaxation time ( $\tau$ ) were determined for each relaxation process of each PU.

### **III. Results and discussion**

#### **1. Main physical properties of 3 PU**

The properties of the three types of PU are summarized in Table 1. The glass transition temperature  $T_{gSD}$  of the SD - microphase - increases by increasing the weight fraction of HS, which confirms the partial miscibility of HS and SS. The melting temperatures  $T_m$  of HD are almost the same for the three PU. From the literature, they are related to the micro-mixing of non-crystalline semi-crystalline hard and soft phases followed by the fusion of crystalline HS [18,19]. The enthalpy related to these endothermal phenomena increases with the HS amount, which indicates an enhanced crystallinity. Indeed, Liff *et al.* [20] confirm that the crystallinity and crystallite perfection increases with HS content due to the perfection of microphase separation between HS and SS. Furthermore Nakamae *et al.* [21] show that an increase of  $\Delta H_m$  of HS must amplify a crystalline morphology within the HS microdomains, which accounts for the HS strengthening and the enhancement in melting endotherm intensity [21].

Table 1 Main physical properties of three studied polyurethanes.

	Composition	HS	Density	$T_{gSD}$	$T_m$	$\Delta H_m$
	MDI/BDO-PTMO	%wt	(g/cm <sup>3</sup> )	(K)	(K)	(J/g)
<b>PU75</b>	PTMO2000	26	1.07	209	430-452	5.13
<b>PU88</b>	PTMO1000	45	1.13	228	420-444	10.13
<b>PU60</b>	PTMO1000	65	1.17	253	422-455	16.11

## 2. Electrostriction properties

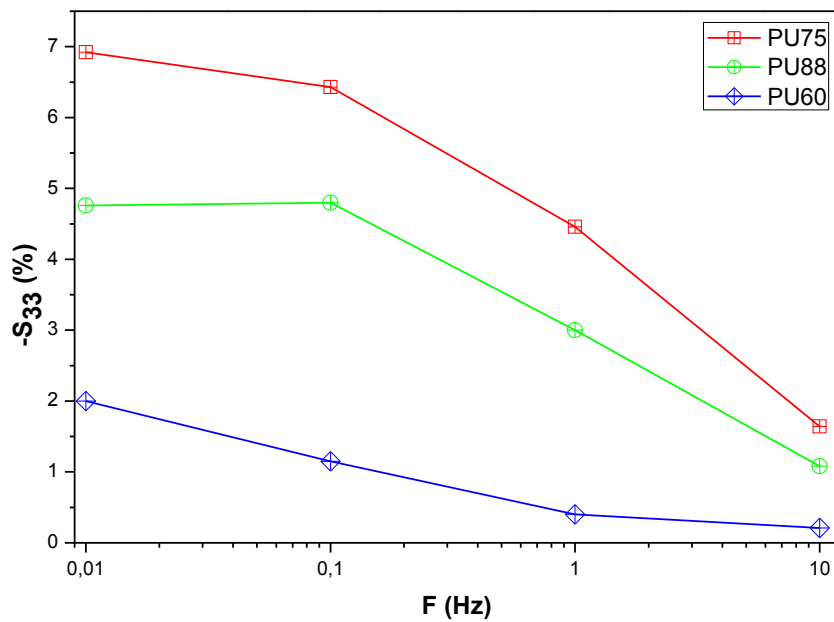


Fig. 3 Variation of the strain thickness at 2 V/ $\mu$ m of 3 PU versus frequency.

Fig. 3 depicts the variations of the strain thickness at 2 V/ $\mu$ m of the 3 PU versus frequency. Experimental  $S_{33}$  values decreases when the frequency is increased. Diaconu *et al.* reported that the thickness strain decreases when the relaxation time is decreased. Moreover the relaxation time also influences on the electrostrictive polymers behavior [22]. Guillot *et al.* [11] have demonstrated that the electrostriction coefficient of PU should decrease when the frequency is increased. Furthermore, Putson *et al.* confirmed that an increase of frequency- for example from 0.1 Hz to 1 KHz- induces a decrease by a factor of 100 the electrostrictive coefficient [23]. The dielectric constant  $\epsilon$  of polyurethane is known to decrease when the frequency is increased because of the decrease of the interfacial Wagner polarization contribution, which exists in all heterogeneous dielectric materials, including multiphase polyurethane [24]. On the contrary, the Young's modulus is known to increase as a function

of frequency because large translational motions are restricted and because relaxation processes can occur when the frequency is increased.

The latter result confirms that the applied frequencies play an interesting role on the electromechanical properties of PU. In addition the frequency can limit the application range of PU polymer as an actuator. On one hand, by decreasing the frequency, the ionic conductivity increases, which can be attributed to charge displacements (which corresponds to dielectric losses). On the other hand by increasing the applied frequency, the Young modulus and the mechanical loss increase as a result of viscoelastic relaxation of PU. Thus, studying the dielectric and viscoelastic properties including relaxation phenomena in a wide range of frequencies and temperatures is necessary to optimize the conditions- applied frequency and temperature- for the use of PU as actuator.

### **3. Dielectric properties of 3PU**

#### **a. Isochronal study**

Fig. 4 presents the real and imaginary parts of dielectric permittivity and the real and imaginary parts of dielectric modulus  $M^*$  at 0.1 Hz and at 1 kHz versus temperature from 180 K to 380 K. As  $M^* = \frac{1}{\epsilon^*}$ , the real dielectric modulus  $M'$  and the dielectric loss modulus  $M''$  can be deduced by the following relations

$$\begin{aligned} M' &= \frac{\epsilon'}{(\epsilon'^2 + \epsilon''^2)} \\ M'' &= \frac{\epsilon''}{(\epsilon'^2 + \epsilon''^2)} \end{aligned} \tag{1}$$

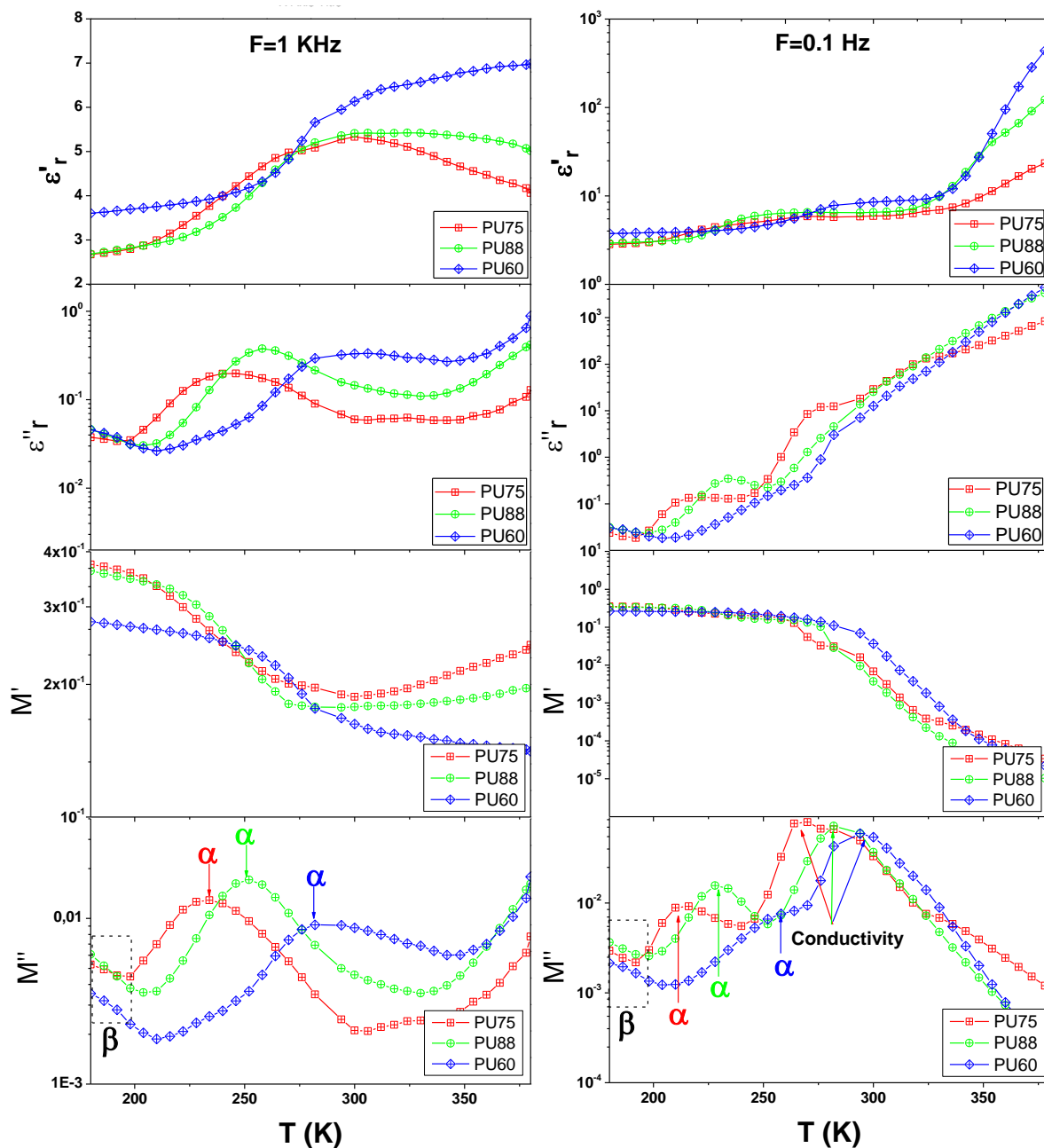


Fig. 4 Evolution of the real and imaginary parts of the dielectric permittivity and the real and imaginary parts of dielectric modulus versus temperature for the 3 PU at 1 kHz (left) and 0.1 Hz (right).

As frequently observed on polymers [25], the dielectric permittivity starts to increase just above  $T_g$  (see Fig. 4). Indeed as the temperature increases, the intermolecular forces between polymer chains are easier to break and the polar groups are freer to move. This behavior corresponds to the  $\alpha$ -relaxation. At temperatures higher than 330 K and depending on the type of polyurethane, the real component of the permittivity  $\epsilon'$  remains constant or starts to decrease due to strong thermal motion which disturbs the dipole orientation [25]. Such

permittivity decrease is mainly observed on PU75. The evolution of  $\epsilon'$  between 300 and 350 K shows that PU88 is the most stable upon the 3 types of PU.

The evolution of  $\epsilon''$  versus temperature shows the dielectric relaxations which are highlighted by  $\epsilon''$  maxima. One important relaxation seen in Fig. 4 is the  $\alpha$  relaxation associated with the motion of the SD microphase [26, 27]. Moreover, a slight increase of  $\epsilon''$  can be observed slightly above 190 K, which is probably related to  $\beta$ -relaxation, as it will be shown in the next section. For the temperature range used here, these relaxations need to be observed at much lower frequencies. These relaxations could be related to the local motion of polymer segments [25, 28, 29, 30]. At higher temperatures, the strong increase of the imaginary dielectric permittivity is related to the Maxwell Wagner Sillars (MWS) interfacial polarization due to accumulation of charges at the interfaces [29, 31]. It corresponds to the ionic conductivity which appears at high temperature - low frequency and which will be discussed later. At 1 kHz, the real part of the dielectric modulus  $M'$  first decreases for temperatures where it is observed a maximum of  $M''$  and after  $M'$  is almost constant. At 0.1 Hz there is an abrupt decrease of  $M'$  showing that the conductivity is the predominant phenomenon.

The examination of loss modulus  $M''$  presented in Fig. 4 allowed the observation of three relaxation mechanisms especially at high temperature and high frequency range. The main advantage of using of the complex modulus,  $M^*$ , rather than  $\epsilon^*$  is that the electrode polarization effect can be better separated from the  $\alpha$ -relaxation and it is a very important and convenient way to analyze and interpret the dielectric relaxation of polymeric materials [32].

### **b. Isothermal Study**

In order to analyze the relaxation processes of the 3 PU, additional measurements were performed over a wide range of temperatures and frequencies. Relaxation spectra are presented as isothermal curves, which display the variation of the imaginary part of  $M''$  in function of the frequency. Fig. 5, 6 and 7 shows the logarithm of the dielectric loss modulus  $M''$  in the function of the frequency and the temperature for PU75, PU88 and PU60, respectively. For sake of clarity, isothermal  $M''$  data of the 3 PU are presented each time in

two different figures: one for high temperatures (270 K to 380 K) and the other one for low temperatures (180 K to 264 K). In the high temperature range,  $M''$  reaches very high values which makes difficult the analysis of the relaxation phenomena around and below  $T_g$ .

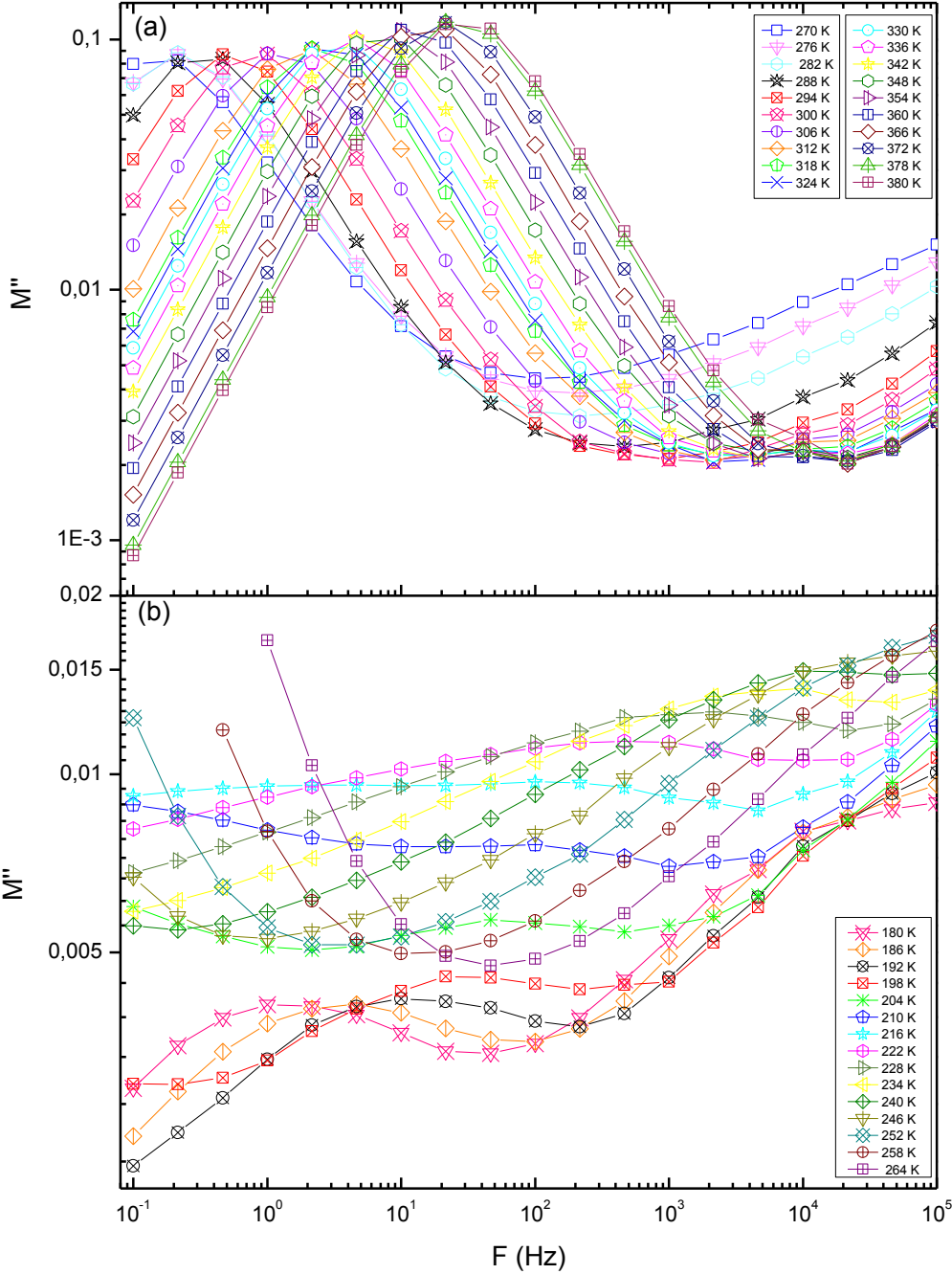


Fig. 5 Electric loss modulus  $M''$  of PU75 versus frequency and temperature; (a) from 270 K to 380 K, (b) from 180 K to 264 K.

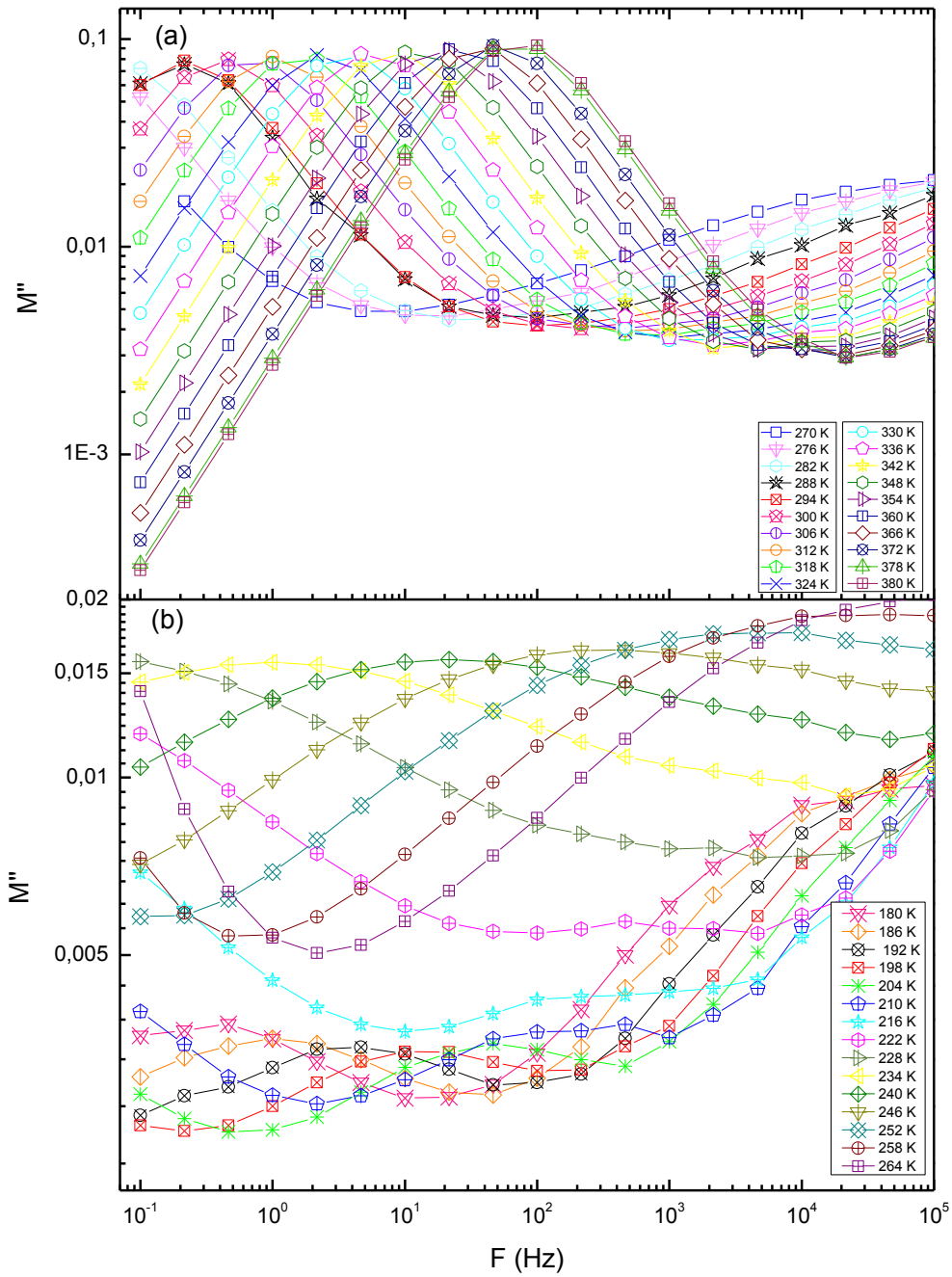


Fig. 6 Electric loss modulus  $M''$  of PU88 versus frequency and temperature; (a) from 270 K to 380 K, (b) from 180 K to 264 K.

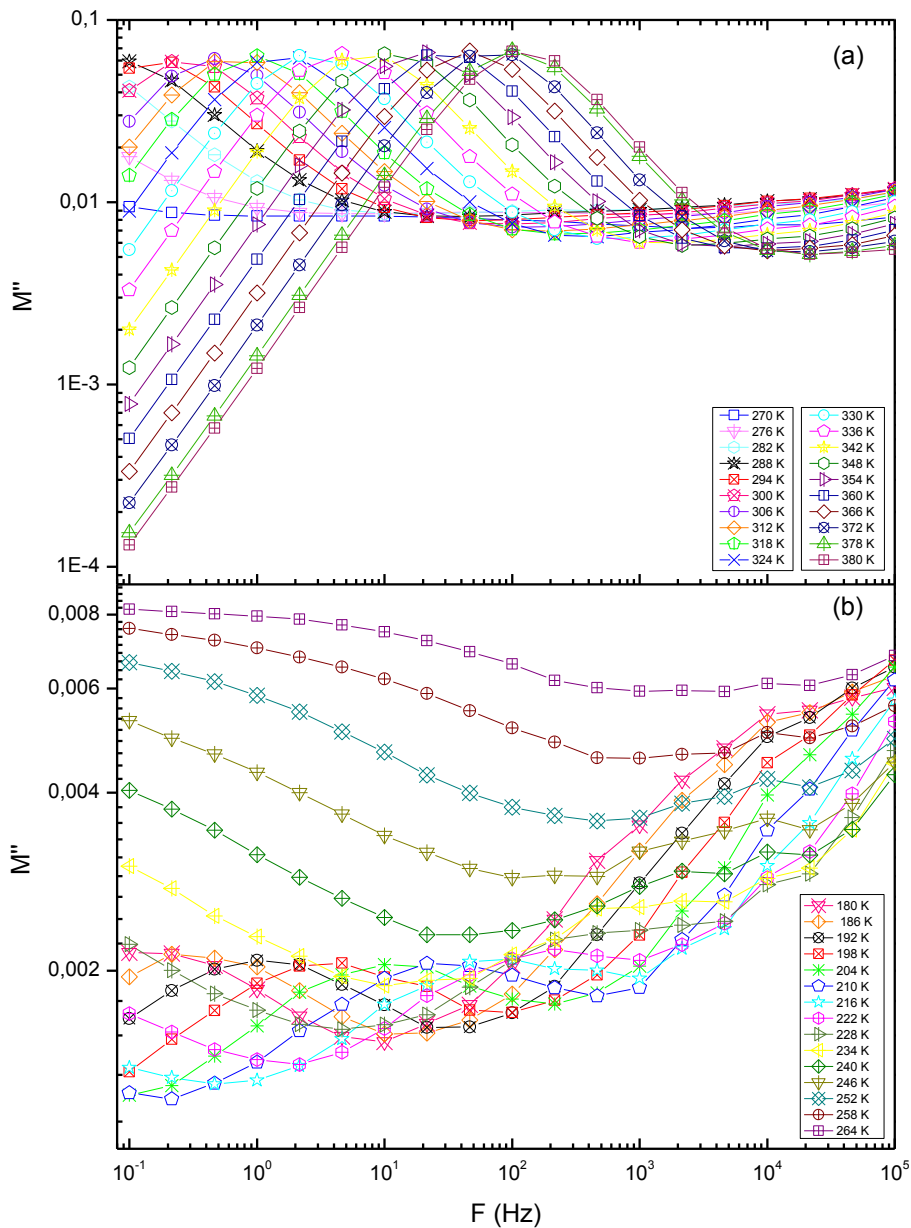


Fig. 7 Electric loss modulus  $M''$  of PU60 versus frequency and temperature; (a) from 270 K to 380 K, (b) from 180 K to 264 K.

Again, three relaxation processes can be observed for the three investigated polymers. At low temperature and/or low frequency, a  $\beta$ -relaxation with very small amplitude can be seen (Fig. 5, 6, 7 (b)). In the temperature-frequency range used here, the  $\gamma$ -relaxation is not visible. It is related to the local motion of  $(CH_2)_n$  [25, 29], and occurs at temperatures lower than the  $\beta$ -relaxation. Figures 5, 6 and 7 highlight the  $\beta$ -relaxation. The  $\beta$ -relaxation has been attributed

in the literature to the motion of the polymer chain segments with attached water molecules [28, 29, 30]. It is present in many water-containing systems, and even if the PU are dried before measurements, some residual water may remain because of strong interactions between HS segments or SS segments and water [32]. The  $\beta$  relaxations are similar for the three PU. At higher temperatures (or lower frequencies) the  $\beta$ -relaxation mechanism is hidden by the beginning of the  $\alpha$ -relaxation of SD [32], and further by the high electrical conductivity.

The  $\alpha$ -relaxation appears in the temperature range of 204 to 264 K only at high frequencies (1 to  $10^5$  Hz) for the 3PU, and has a larger amplitude than the  $\beta$ -relaxation as seen in Fig. 5b, 6b, 7b. This relaxation corresponds to a longer scale segmental motion, and is associated with the glass transition [26, 27]. As for  $T_g$ , the  $\alpha$ -relaxation shifts to higher temperatures with increasing HS amounts. For PU60 the  $\alpha$ -relaxation cannot be easily analyzed because it is superimposed to the conductivity effect, which is especially large in that case, as discussed below.

A third very strong relaxation process starts at 270 K at low frequency Fig. 5a, 6a, and 7a. This phenomenon is very sensitive to frequency and shifts to higher frequencies when increasing the temperature. It corresponds to high values of the DC conductivity. Karabanova *et al* discussed such high values of the dielectric loss  $M''$  at low frequencies and high temperatures [26, 33]. This relaxation phenomenon is attributed to the existence of ionic polarization in polyurethane network due to "free" charge motion within the material.

For the different relaxation processes, using  $M''(T,f)$  data, and more precisely the frequencies  $f_M$  at which  $M''$  passes through a maximum, it is easy to determine the so-called relaxation time  $\tau = 1/2\pi f_M$  and to get a set of  $\tau(T)$ . It is usual to plot  $\log(\tau)$  versus  $1/T$  (in a so-called Arrhenius plot), and to determine the equation of the corresponding curve. If the curve is a straight line, then the relaxation time follows the Arrhenius equation:

$$\tau = \tau_0 \cdot \exp \frac{E}{k_B T} \quad (2)$$

Where  $\tau_0$  is the pre-exponential time,  $k_B$  the Boltzmann constant and  $E$  the activation energy. For the cooperative  $\alpha$ -relaxation, the temperature dependence of  $\tau$  is often described by the Vogel-Tammann-Fulcher (VTF) equation

$$\tau = \tau_0 \cdot \exp \frac{B}{(T-T_0)} \quad (3)$$

Where  $\tau_0$  is the pre-exponential time, B is an activation parameter and  $T_0$  is the ideal glass transition temperature (or the Vogel temperature) [26, 33], ( $T_0$  being 40 K lower than  $T_g$ ) [33].

Fig. 8 shows semi-logarithmic plot of  $\tau$  against reciprocal temperature,  $1/T$ , for the 3 PU. The curves are the fits of equations (2) and (3) for the  $\beta$  and  $\alpha$  relaxations respectively. The experimental points are also included in the plots.

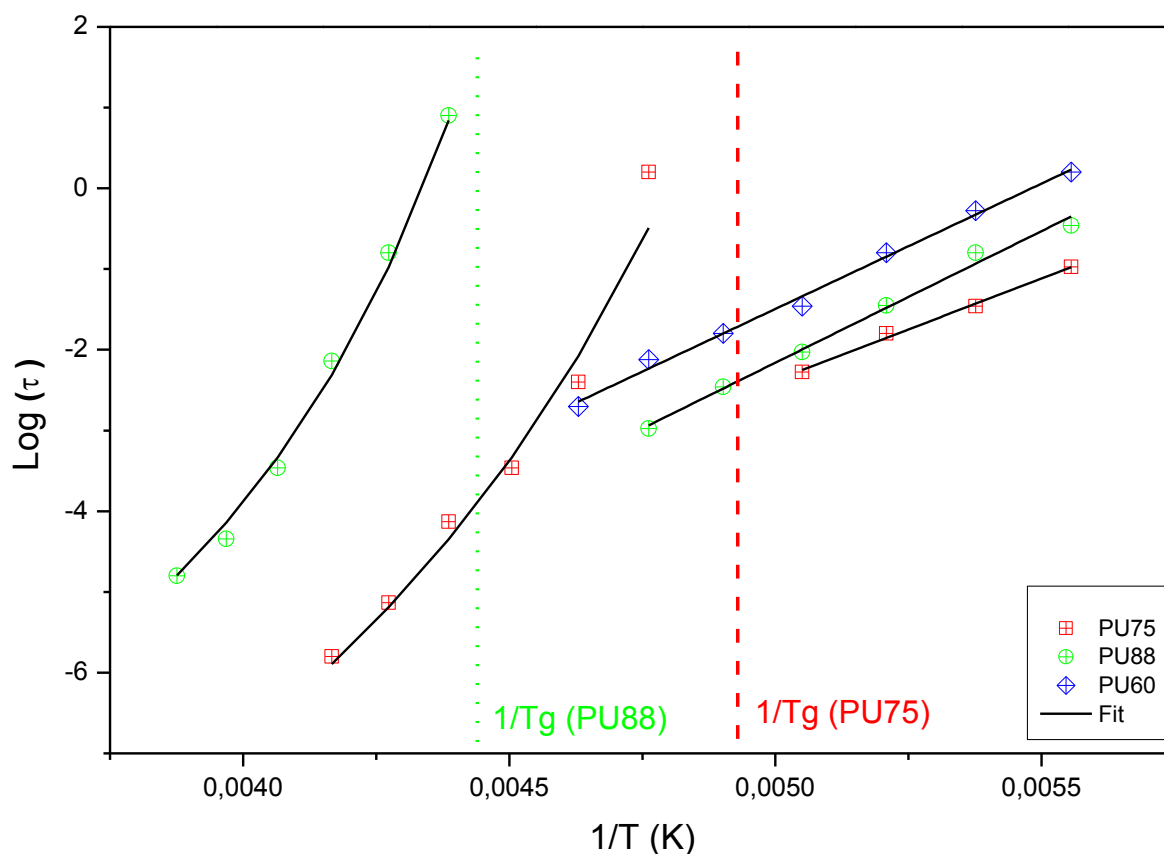


Fig. 8  $\log(\tau)$  versus  $1/T$  for  $\alpha$  and  $\beta$  relaxations for the 3 PU.

The results of the fitting procedure are listed in Table 2.

Table 2 Parameters of Arrhenius equation (equation (2)) for the  $\beta$ -relaxation, and of VTF equation for the  $\alpha$ -relaxation (VTF equation, equation (3)). The parameters related to the  $\alpha$ -relaxation could not be measured on PU60 because of the large conductivity.

		<b>PU75</b>	<b>PU88</b>	<b>PU60</b>
<b><math>\beta</math>-relaxation</b>	$E$ (kJ/mol)	49	63	60
	$\tau_0$ (S)	$10^{-15}$	$10^{-18}$	$10^{-17}$
<b><math>\alpha</math>-relaxation</b>	$B$ (K)	1400	900	N.D.
	$T_0$ (K)	165	195	N.D.
	$\tau_0$ (s)	$10^{-15}$	$10^{-12}$	N.D.

The  $\beta$  relaxation is described by practically the same parameters  $E$  and  $\tau_0$  for the three materials. The relaxation times of the  $\beta$ -processes are not significantly affected by the HS content and the values of the activation energies are similar to other reported values [34].

For the  $\alpha$ -relaxation, it is striking that the VTF parameters are different for sample PU75 compared with PU88. The results indicate that the cooperative primary  $\alpha$  process is more sensitive to morphology changes than the local secondary  $\beta$  process [26].

The fitting parameters have reasonable values for all three samples, e.g. for  $T_0$  is 165 K for PU75 and 195 K for PU88 Table 2, in reasonable agreement with  $T_0$  being about 40 K lower than  $T_g$  [26, 34].

$T_g$  can be estimated from the segmental relaxation by extrapolation of the VTF fit to  $\tau = 100$  s.  $T_g$  equals to 207 K and 226 K for PU75 and PU88 respectively. These values are in good agreement with experimental data obtained by DSC measurement (see Table 1).

### c. Conductivity

Fig. 9 displays the evolution of the real part of conductivity of the 3PU in function of the frequency, for temperature ranging from 270 K to 378 K.

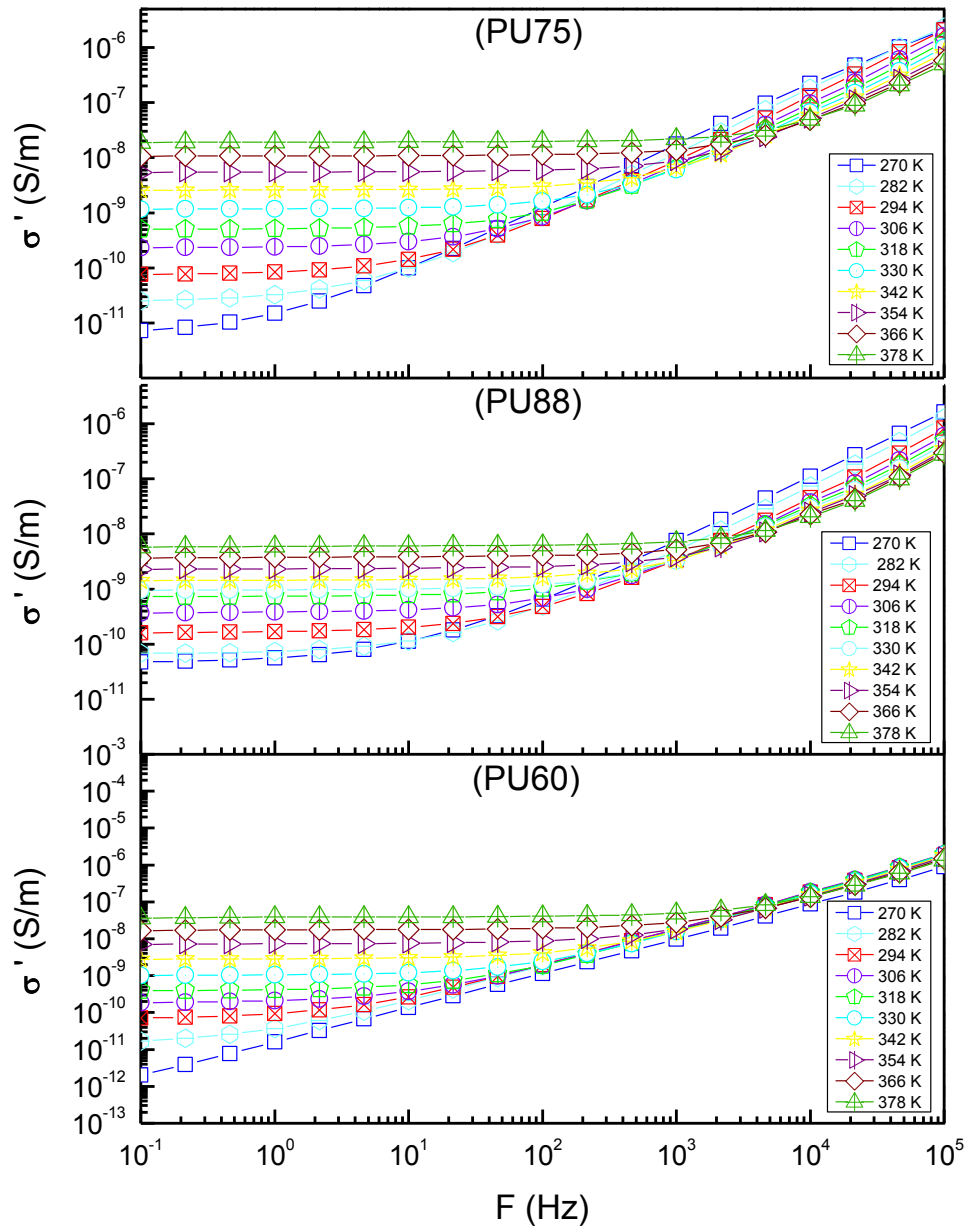


Fig. 9 Real part of conductivity versus frequency measured at different temperatures.

Two regions can be observed from the curves: one for which the conductivity is almost independent on the frequency in the low frequency range. This corresponds to a resistive behavior and is attributed to charge displacements (which corresponds to dielectric losses),

and another one for which the conductivity increases with the frequency and corresponds to almost purely capacitive behavior. The dc conductivity  $\sigma_{dc}$ -for each sample- is considered to be equal to the value of  $\sigma(f)$ , at the lowest measured frequency  $f=10^{-1}$  Hz in the present case, in the temperature range where the low-frequency plateau occurs. If this electrical conductivity  $\sigma_{dc}$  comes from ions flow, the corresponding current is driven by diffusion process, and as expected, the  $\sigma_{dc}$  increases with increasing temperatures. Such ions are probably impurities introduced during the polymerization process of polyurethane. In Fig. 10 both Arrhenius plots drawn either from the maxima of the  $M''$  peak or from  $\log(\sigma_{dc})$  -at  $f=10^{-1}$  Hz and for all temperatures- versus reciprocal temperature are displayed for the three PU. Curves of Fig. 5a, 6a, and 7a were used for the calculation of the activation energy of ionic conductivity  $E_c$ , and  $\tau_{0c}$  [33, 34] and curves of Fig. 10 were used for the determination of  $E_{dc}$ . As it can be in seen in Fig. 10, both curves have very similar slopes. Thus, as expected, the apparent activation energies measured from these two set of curves lead to same values.

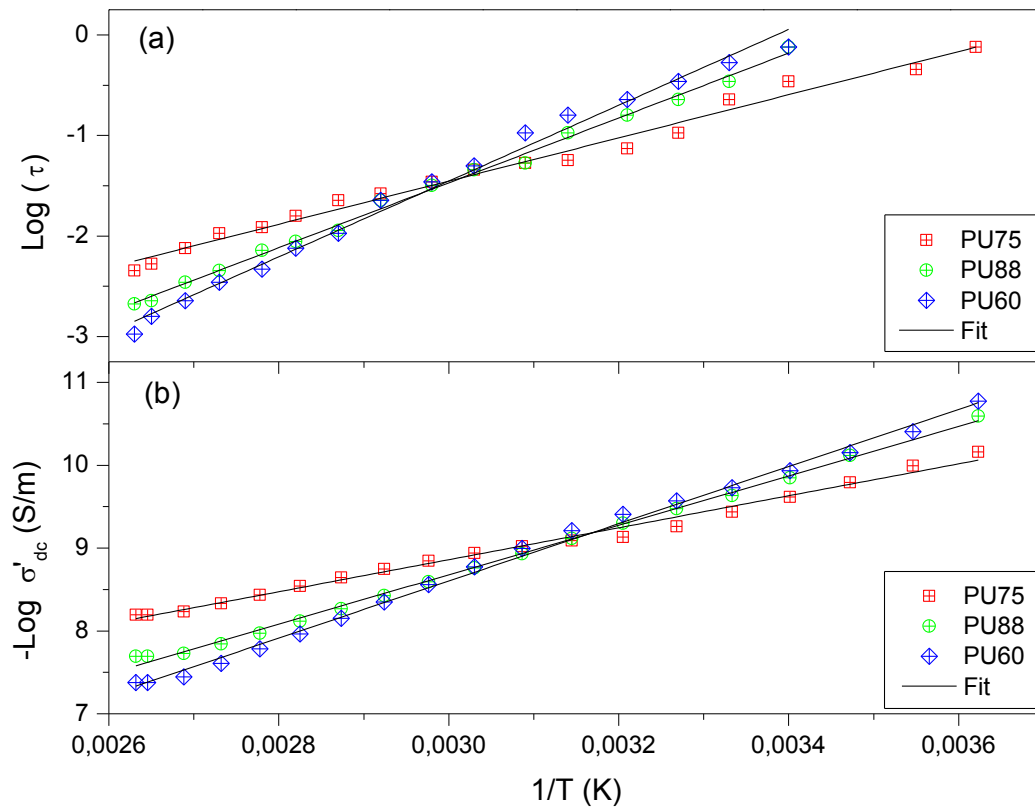


Fig. 10 Arrhenius plot of conductivity relaxation, obtained from  $M''$  maxima (a) and from  $\sigma_{dc}$  conduction measurements (b).

The results of the fitting procedure are listed in Table 3.

Table 3 Parameters of Arrhenius equation (equation (2)) for the conductivity relaxation,  $E_c$  activation energy and  $\tau_{0c}$  pre-exponential relaxation time obtained from  $M''$  maxima (a) and  $E_{dc}$  activation energy from  $\sigma_{dc}$  conduction measurements (b) (see Fig. 9).

		<b>PU75</b>	<b>PU88</b>	<b>PU60</b>
<b>Conductivity relaxation</b>	$E_c$ (kJ/mol)	41	62	75
	$\tau_{0c}$ (S)	$10^{-7}$	$10^{-11}$	$10^{-12}$
	$E_{dc}$ (kJ/mol)	39	57	67

It is worthy to notice that in the temperature-frequency window, the curves appear as straight lines and their slopes lead to the apparent activation energy of the conduction mechanism. As expected for each PU, the data lead to the same activation energy within the measurement uncertainty (see Table 3). It seems to be related in these polyurethanes to a conductivity of ionic type only. Furthermore this activation energy increases by increasing the weight fraction of HS Fig. 10. Two remarks have to be done. First of all, very long pre-exponential times such

as  $\tau_{0c}$  for PU75 are incompatible with a two wells relaxation model which are known to follow the Arrhenius law: their order of magnitude should be around the Debye time, i.e.  $10^{-13}$ s. On the other hand, if the conductivity is governed by diffusion processes of the macromolecules, thus a VTF type behavior is expected. In the high temperature range and narrow frequency range, the VTF equation leads to almost linear curves. If this is the case, the extrapolation of such function to infinite temperatures has thus no meaning, and neither the pre-exponential time. This may explain the very high value for  $\tau_{0c}$  in Table 3 for PU75.

Moreover, it is noteworthy that the conductivity temperature dependence is almost the same for the 3 PU and relatively small. The 3 PU exhibits the same conductivity around room temperature. It is probable that the conductivity occurs mostly in the soft phase, and strongly depends on the presence of impurities which in turn should depends on the polymerization step. The diffusion processes are slower in PU60 because of its higher  $T_{gSD}$ , which is consistent with a higher DC conductivity activation energy. However, this weak temperature dependence leads to the fact that for PU60, the DC conductivity strongly overlaps with the  $\alpha$ -process.

#### IV. Conclusions

The purpose of this study was to provide as many pieces of information as possible on the dielectric behaviour of polyurethane frequently used for their rather strong electrostrictive properties.

In order to determine in which temperature - frequency domain they have their maximum efficiency, and minimum electrical loss, the relaxation maps have been determined for 3 polyurethanes of similar chemical compositions but containing different fraction of hard and soft segments. A particular attention has been paid (i) on one of their secondary relaxations (just below  $T_g$  of the soft phase) so-called  $\beta$ -relaxation, (ii) on their  $\alpha$ -relaxation corresponding to  $T_g$  of the soft phase and (iii) on a relaxation which results from the conductivity. It is worthy to notice that the  $\beta$ -relaxations behave in a very similar way for the

3 PU, and is probably associated to interactions of polar chain segments with residual water. On the contrary, the  $\alpha$ -relaxation is very sensitive on the composition and shifts towards high temperature with increasing content of hard segments. Finally, the DC conductivity analysis through the study of the complex dielectric modulus shows that it is comparable for the 3 PU, and that probably most of its contribution comes from the soft phase, as it disappears for temperatures lower than  $T_g$ . For PU60, the overlap of the soft phase  $\alpha$  process with the conductivity relaxation made impossible to determine with precision the characteristics of the  $\alpha$ -relaxation. The consequence is that losses come from both the  $\alpha$  and the DC processes for PU60, which in turn would decrease its efficiency in energy conversion (both for actuation or energy harvesting applications). PU88 and PU75 show a better stability of the dielectric properties at temperatures above the ambient temperature, making them more suitable for energy conversion applications.

In order to optimize the composition of such materials, not only the dielectric behaviour must be analysed, but also their mechanical properties, as both behaviours are involved for energy conversion. Such mechanical analysis, performed on the 3 same PU is under study. The relations between the dielectric, mechanical and electrostrictive properties in PU will also be discussed.

## **Acknowledgments**

The author acknowledges the financial support of the French Agence Nationale de la Recherche (ANR), under grant NAPOLECO (ANR- 2010-INTB-910-01).

## References

- [1] Bar-Cohen Y. *Electroactive Polymer (EAP) Actuators as Artificial Muscles (Reality, Potential and Challenges)*. SPIE Press. Bellingham. 2004.
- [2] Watanabe M, Hirai T, Suzuki M, Yoichi M. Electric conduction in bending electrostriction of polyurethanes. *Appl. Phys. Lett* 1999; 18: 2717–2719.
- [3] Su J, Zhang Q M, Kim C H, Ting R Y, Capps R J. Effects of transitional phenomena on the electric field induced strain–electrostrictive response of a segmented polyurethane elastomer. *Appl. Polym. Sci.* 1997; 65: 1363–1370.
- [4] Guiffard B, Seveyrat L, Sebald G, Guyomar D. Enhanced electric field induced strain in non percolative carbon nanopowder / polyurethane composites. *J. Phys. D: Appl. Phys.* 2006; 14:3053- 3057.
- [5] Guelcher S A, Gallagher K M, Didier J E, Klinedinst D B, Doctor J S, Goldstein A S, Wilkes G L, Beckman E J, Hollinger J O. Synthesis of biocompatible segmented polyurethanes from aliphatic diisocyanates and diurea diol chain extenders. *Acta Biomater.* 2005; 4: 471-484.
- [6] Petrović Z S, Javni I. The effect of soft-segment length and concentration on phase separation in segmented polyurethanes. *J. Polym.Sci. B Polym. Phys.* 1989; 27: 545–560. doi: 10.1002/polb.1989.090270305.
- [7] Lin J R, Chen L W. Study on shape-memory behaviour of polyether-based polyurethanes. II. Influence of soft-segment molecular weight. *Appl. Polym. Sci.* 1998; 69: 1575–1586. DOI: 10.1002/(SICI)1097-4628(19980822)69:8<1575:AID-APP12>3.0.CO;2-U.
- [8] Chattopadhyay D K, Raju K V S N. Structural engineering of polyurethane coatings for high performance applications. *Prog. Polym. Sci.* 2007; 32: 352–418. DOI : 10.1016/j.progpolymermsci.2006.05.003
- [9] Byung K K, Sang Y L. Polyurethanes having shape memory effects. *Polymer.* 1996; 37:5781-5793.DOI: 10.1016/S0032-3861(96)00442-9
- [10] Sudipto D, Iskender Y, Emel Y, Bora I, Ozgul T, Frederick L B, Garth LW. Structure property relationships and melt rheology of segmented,non-chain extended polyureas:

- Effect of soft segment molecular weight. *Polymer*. 2007; 48:2 90-301. DOI:10.1016/j.polymer.2006.10.029.
- [11] Guillot F M , Balizer E. Electrostrictive effect in polyurethanes. *Journal of Applied Polymer Sci.* 2003; 89: 399-404. DOI: 10.1002/app.12096.
- [12] Korley LT J, Pate B D, Thomas E L, Hammond P T. Effect of the degree of soft and hard segment ordering on the morphology and mechanical behavior of semicrystalline segmented polyurethanes. *Polymer*. 2006; 47: 3073-3082. DOI: 10.1016/j.polymer.2006.02.093.
- [13] Pichon P G, David L, Mechin F, Sautereau H. Morphologies of Cross-Linked Segmented Polyurethanes. Evolution during Maturation and Consequences on Elastic Properties and Thermal Compressive Fatigue. *Macromolecules*. 2010; 43: 1888–1900. DOI: 10.1021/ma901602y
- [14] Petrovic Z S, Ferguson J. Polyurethane elastomers. *Prog. Polym. Sci.* 1991; 16: 695-836.
- [15] Laity P R, Taylor J E, Wong S S, Khunkamchoo P, Norris K, Cable M , Andrews G T, Johnson A F, Cameron R E . A review of small-angle scattering models of random segmented poly(ether-urethane) copolymers. *Polymer*. 2004; 45: 7273-7091. DOI: 10.1016/j.polymer.2004.08.033.
- [16] Eun A K, Han S L. Effect of molecular shape of diisocyanate units on the microscopic/macrosopic phase separation structure of polyurethanes. *J. Polym. Sci. Polym. Phys.* 2011; 49: 890–897. DOI: 10.1002/polb.22264.
- [17] Yang C Z, Grasel TG, Bell J L, Register R A, Cooper S L. Carboxylate containing chain-extended polyurethanes. *J. Polym. Sci. B Polym. Phys.* 1991; 28: 581–588. DOI: 10.1002/polb.1991.090290507.
- [18] Koberstein J T, Russell T P. Simultaneous SAXS-DSC Study of Multiple Endothermic Behavior in Polyether-based Polyurethane Block Copolymers. *Macromolecules*. 1986; 19: 714-720. DOI: 10.1021/ma00157a039.

- [19] Lapprand A, Mechin F, Pascault J P. Synthesis and properties of self-crosslinkable thermoplastic polyurethanes. *J. Appl. Polym. Sci* 2007; 105: 99-113. DOI: 10.1002/app.26086.
- [20] Liff SM, Kumar N, McKinley G. High- performance elastomeric nanocomposites via solvent -exchange processing. *Nature Materials*. 2007; 6: 76-83.
- [21] Nakamae K, Nishino T, Asaoka S, Sudaryanto. Microphase separation and surface properties of segmented polyurethane - Effect of hard segment content. *Int. Journal of Adhesion and Adhesives*. 1996; 16: 233-239.
- [22] Diaconu I, Dorohoi D. Properties of polyurethane thin films, *J. Optoelectron. Adv. Mater*. 2005; 7:921-924.
- [23] Putson C. Energy conversion from electroactive materials and modeling of behaviour on these materials. PhD Thesis, 2010, INSA Lyon, France.
- [24] Guyomar D, Cottinet P J, Lebrun L, Putson C, Yuse K, Kanda M, Nishi Y. The compressive electrical field electrostrictive coefficient  $M_{33}$  of electroactive polymer composites and its saturation versus electrical field, polymer thickness, frequency, and fillers. *Polym. Adv. Technol*. 2012; 23: 946–950.
- [25] Ahmad Z. Polymer Dielectric Materials, Dielectric Material, Dr. Marius Alexandru Silaghi (Ed.), 2012, ISBN: 978-953-51-0764-4, InTech, DOI: 10.5772/50638.
- [26] Pissis P, Kanapitsas A, Savelyev Y V, Akhranovich E R, Privalko E G, Privlako V P. Influence of chain extenders and chain end groups on properties of segmented polyurethanes, II. Dielectric study. *Polymer*. 1998; 39: 3431-3435. DOI:10.1016/S0032-3861(97)10100-8.
- [27] Boiteux G, Seytre G, Cuve L, Pascault J P. Dielectric studies of segmented polyurethanes based on polyolefine: relations between structure and dielectric behavior. *J. Non-Cryst. Solids*. 1991; 133: 1131-1135. DOI: 10.1016/0022-3093(91)90739-S.
- [28] Zhang Q M, Su J, Kim C H. An experimental investigation of electromechanical responses in a polyurethane elastomer. *J. Appl. Phys*. 1997; 81:2770-2776. DOI: 10.1063/1.363981.

- [29] Kanapitsas A, Pissis P. Dielectric relaxation spectroscopy in crosslinked polyurethanes based on polymer polyols. *Eur. Polym. J.* 2000; 36: 1241–1250. DOI: 10.1016/S0014-3057(99)00167-6.
- [30] Castagna A M, Fragiadakis D, Hyungki L, Choi T, Runt J. The Role of Hard Segment Content on the Molecular Dynamics of Poly(tetramethylene oxide)-Based Polyurethane Copolymers. *Macromolecules.* 2011; 44 : 7831-7836. DOI: 10.1021/ma2017138.
- [31] Hanafy T A. Dielectric and Electric Modulus Behavior of Chlorinated Poly(Vinyl Chloride) Stabilized with Phenyl Maleimide. *Adv. Mater. Phys. Chem.* 2012; 2: 255-266. DOI: 10.4236/ampc.2012.24038.
- [32] Pissis P, Apekis L, Christodoulides C, Niaounakis M, Kyritsis A , Nedbal J. Water effects in polyurethane block copolymers. *J. Polym. Sci Part B: Polym. Phys.*1996; 34:1529-1539. DOI:10.1002/(SICI)1099-0488(19960715)34:9<1529::AID-POLB1>3.0.CO;2-G.
- [33] Karabanova L V, Boiteux G, seytre G, Stevenson I, Gain O, Hakme C, Lutsyk E D, Svyatyna A. Semi-interpenetrating polymer networks based on polyurethane and poly(2-hydroxyethyl methacrylate): Dielectric study of relaxation behavior. *J. Non-Cryst. Solids.* 2009; 3551453-1460. DOI:10.1002/app.12592.
- [34] Georgoussis G, Kyritsis A, Pissis P, Savelyev Y V, Akharonovich E R, Privalko E G, Privalko V P. Dielectric studies of molecular mobility and microphase separation in segmented polyurethane. *Eur. Polym.* 1999; 35: 2007- 2017. DOI : 10.1016/S0014-3057(98)00288-2.